

Electrical characterization of GaN/ALN heterostructures grown by molecular beam epitaxy on silicon substrates

J.B. Rojas-Trigos

*Instituto Politécnico Nacional, Centro de Investigación en Ciencia Aplicada y Tecnología Avanzada.
Legaria No. 694 Colonia Irrigación, 11500 México D.F., México.*

M. López-López, M.A. Venegas

*Departamento de Física, Centro de Investigación y Estudios Avanzados del Instituto Politécnico Nacional,
Avenida IPN No. 2508 Colonia San Pedro Zacatenco, 07360 México D.F., México.*

G.S. Contreras-Puente, D. Jiménez-Olarte

*Instituto Politécnico Nacional, Departamento de Física, Escuela Superior de Física y Matemáticas,
Avenida IPN Edificio 9, Unidad Profesional Adolfo López Mateos, Zacatenco, 07738 México D.F., México.*

G. Santana-Rodríguez

*Instituto de Investigaciones en Materiales, Universidad Nacional Autónoma de México,
Circuito Exterior, Ciudad Universitaria, Colonia Coyoacán, 04510 México D.F., México.*

Received 26 August 2014; accepted 6 November 2015

In this paper, *n*-type gallium nitride thin films were grown on *p*-type and *n*-type silicon substrates by Molecular Beam Epitaxy technique, employing an aluminum nitride layer as an insulator buffer coating. The samples constitute primary semiconductor-insulator-semiconductor or SIS heterostructures, on which silver electrical contacts were deposited superficially by sputtering for electrical characterization purposes. The current intensity vs. voltage curves, charge carriers density, diffusion coefficient and mobility of charge carriers were determined in darkness conditions. Under AM1.5 homogenous illumination, the samples exhibited relatively large open-circuit voltage values, but low values for energy conversion efficiencies. Additionally, the dependency in photon energy of the open-circuit voltage was determined, in the range 1.77 eV to 4.13 eV, showing a minimum in the energy corresponding to the GaN energy band gap. Finally we discuss the prevailing charge transfer mechanism.

Keywords: Electrical characterization; gallium nitride; Hall effect; molecular beam epitaxy; semiconductor-insulator-semiconductor structures

PACS: 73.40 Ty; 73.50 Pz; 73.61 Ey; 06.60 Ei

1. Introduction

The study of III-N semiconductors alloys family, particularly nitrides of indium, gallium and aluminum (InN, GaN, and AlN) has become an exciting research area because of its wide technological applications. Due to the values of their energy band gaps (0.7 eV, 3.5 eV and 6.3 eV respectively), the growth of multilayer thin films and nanostructures systems, and/or their ternary alloys allows to explore or research both, narrow and wide wavelength ranges, from the mid infrared (mid-IR) to deep ultraviolet (deep-UV) regions [1,2]. Among the most prominent applications are: Radiation detection, light emitting diodes (LED's) and laser diodes (LD's), photovoltaic (PV) cells and solid state lighting, for example [3-5]. For the study of the physical properties, such as thermal, optical, and electrical properties, as well as for the structural and chemical characterization of the III-N semiconductor family, a variety of characterization techniques and methods are commonly used, such as: Photoluminescence (PL) response measurements, Photothermal (PT) and Photoacoustic Spectroscopy (PAS) characterization techniques, X-ray diffraction (XRD), Reflection High-Energy Electron Diffraction (RHEED), Scanning Electron

Microscopy (SEM), Energy-Dispersive X-ray Spectroscopy (EDS), Hall Effect measurements (HEM), among others. These techniques are non-invasive, no destructive tests and do not demand special sample preparation, with the exception of the electrical characterizations which needs the deposition of Ohmic electrical contacts.

The Molecular Beam Epitaxy (MBE) of GaN directly in Si substrates presents several difficulties, like the formation of SiN amorphous layer at the interface due to the strong reaction of the Nitrogen atoms with the Si substrate [6,7]. In order to overcome this problem intermediate buffer layer, such as AlN, have been employed leading to an improvement on the structural and optical properties of the GaN [8]. In this work, we report the electrical characterization of GaN films grown by MBE on silicon (Si) wafers employing an AlN thin buffer. The electrical properties of GaN/AlN/Si heterostructures were studied by means of Hall Effect and Current Intensity vs. Voltage (I-V) curves measured at room temperature.

2. Samples preparation

Three groups of samples, labeled here as M1, M2, and M3, of thin films of GaN were grown by the MBE technique in

TABLE I. Growth parameters used for the group sample.

Sample	GaN Layer					AlN Layer				
	T_{subs} °C	T_{Ga}	d_{GaN} μm	P_{Ga} $\times 10^7$ torr	P_{MBE}	T_{sus} °C	T_{Al}	d_{AlN} nm	P_{Al} $\times 10^7$ torr	P_{MBE}
M1	750	970	0.6	4.8	45	850	1133	46.0	3.3	43
M2	730	970	0.6	4.8	40	850	1133	46.0	3.3	42
M3	800	972	1.4	5.4	48	850	1127	27.6	3.3	46

a Riber C21 system, equipped with a radio frequency gas source for supplying atoms of nitrogen from molecular form. As substrates, a 380 μm thickness low-resistivity *p*-type silicon (Si) was used for samples M1 and M2; meanwhile for sample M3, a 500 μm thickness high-resistive, *n*-type Si wafer was employed. All the substrates had the (111) orientation, and were previously characterized by HEM, in darkness conditions at room temperature. On each of the substrates, an AlN layer was grown as insulator buffer layer, previous to the growth of the GaN layer, unintentionally doped as *n*-type due to native N-vacancy defects [9-11], and a possible diffusion of Si donors from the substrate to the AlN and GaN layers, during the growth process [12]. In Table I, the used growth parameters are reported.

Here, T_{sub} is the substrate temperature; T_{Ga} and T_{Al} are the temperatures of the Knudsen cells of Ga, and Al cells, respectively; and d_{GaN} and d_{AlN} are the nominal thickness of the GaN and AlN layers respectively. P_{MBE} is the pressure of the MBE chamber during growth; and P_{Ga} and P_{Al} are the beam equivalent pressure of the Knudsen cells of Ga and Al, respectively. From each case, square sections (with an area of 0.25 cm^2) were cut using a diamond cutting wheel. The samples were cleaned, firstly in cyclohexane, secondly in acetone (95%), after that in isopropyl alcohol (95%) and finally washed in deionized water (DI), in an ultrasonic bath during 15 minutes for each step. For all samples, square-shaped silver (Ag) contacts were deposited, near as possible to the corners of the samples, directly on the surface of the GaN layer, using a sputtering deposition system (Denton Desk IV Sputter). The deposition time was 1.5 minutes, obtaining electrical contacts with thickness in the range of 15 nm to 22 nm, and having an area of $\sim 1 \text{ mm}^2$. Also, a thin layer of Ag was deposited (by the same method) on the exposed back surface of the Si substrates. The upper and lower contacts allow electrical measurements in the GaN layer and across the axial direction of the sample. The electrical contacts shows good mechanical adherence and shape definition. Figure 1 shows a schematic drawing of the samples structure, and the positions of the electrical contacts.

From spectral reflectance measurements in the range of 350 nm to 700 nm, the average thickness of the GaN layer was determined [13,14] for each sample group, finding differences less than 7% between the nominal thicknesses and those obtained by reflectance measurements.

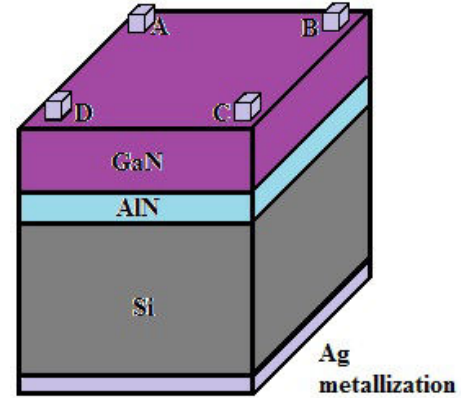


FIGURE 1. Schematic representation of the grown heterostructures. The uppercase letters identify the electrical contacts.

3. Electrical characterizations

Two kinds of electrical characterizations were performed at room temperature: HEM and I-V measurements of the substrate and GaN layers in darkness conditions, to obtain their individual electrical parameters; and I-V and open-circuit voltages measurements, under homogenous illumination conditions, to evaluate the energy conversion efficiency and spectral response, of the samples heterostructures.

3.1. Electrical measurements: Darkness conditions

By means of a Hall Effect Measurement System (ECOPIA, HMS-3000) the electrical parameters of the GaN and substrate were determined, using the van der Pauw geometry [15], applying a current intensity of 1 mA in the presence of a uniform magnetic flux density of 0.55 T. Since the measurements were done in darkness conditions, there is no influence of photogenerated charge carriers in the results. Tables II and III summarize the results from the HEM characterization.

Where, n_c , μ_c , ρ , R_H and D_c stands for the charge carrier concentration, charge mobility, electrical resistivity, average Hall coefficient and charge carrier diffusion coefficient, respectively. From Tables II and III, it can be seen that the GaN layers exhibit larger charge carrier concentration and lower electrical resistivity values than their correspond-

TABLE II. Hall Effect results of the GaN layer of the samples group, in darkness condition at room temperature.

	GaN layer		
	M1	M2	M3
$ n_c $			
cm^{-3}	8.3×10^{18}	6.0×10^{18}	1.1×10^{18}
μ_c			
$\text{cm}^2/(\text{Vs})$	17.3	29.1	34.2
ρ			
$\Omega \cdot \text{cm}$	4.4×10^{-2}	3.6×10^{-2}	1.6×10^{-1}
R_H			
$\text{cm}^3 \cdot \text{C}^{-1}$	-0.75	-1.0	-5.6
D_c			
$\text{cm}^2 \cdot \text{s}^{-1}$	0.44	0.75	0.88

TABLE III. Hall Effect results of the substrates, in darkness condition at room temperature.

	Substrates	
	<i>p</i> -type	<i>n</i> -type
$ n_c $		
cm^{-3}	1.5×10^{15}	1.1×10^{12}
μ_c		
$\text{cm}^2/(\text{Vs})^{-1}$	8.4×10^2	1.6×10^3
ρ		
$\Omega \cdot \text{cm}$	11.4	3.4×10^3
R_H		
$\text{cm}^3 \cdot \text{C}^{-1}$	4.3×10^3	-5.5×10^6
D_c		
$\text{cm}^2 \cdot \text{s}^{-1}$	9.5	41.7

ing substrates, which is consistent with reported observations in similar heterostructures [16,17]. The I-V measurements show that the behavior of the GaN layer is not perfectly Ohmic, but close to this behavior in the range of -5 mA to 5 mA (see Fig. 2).

3.2. Electrical measurements: Homogenous illumination conditions

To obtain the electrical response of the samples under homogenous illumination, two sets of data are here reported: (a) The I-V curves under AM1.5 illumination, and (b) The open-circuit voltage dependence on the excitation wavelength. Figure 3 schematizes the experimental setups employed.

The AM1.5 illumination was acquired by a solar simulator (Oriel-Newport mod. 91160), with an irradiance of $140 \text{ W} \cdot \text{cm}^{-2}$. The monochromatic illumination was acquired by passing the output radiation from a 900 W Xe arc lamp,

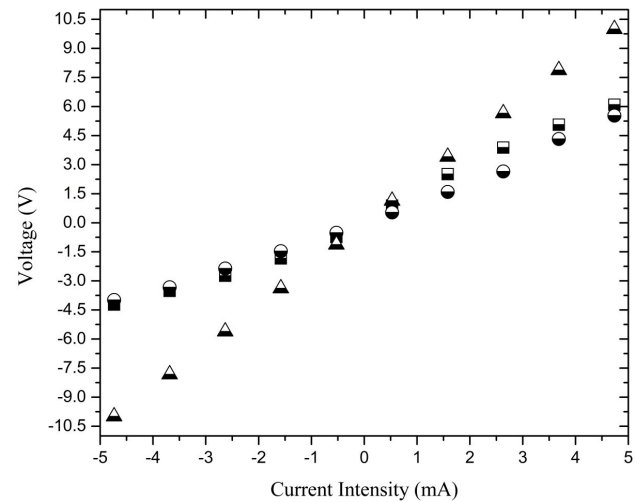


FIGURE 2. I-V curves of samples M1 (half-full squares), M2 (half-full circles), and M3 (half-full up triangles), through AB trajectory.

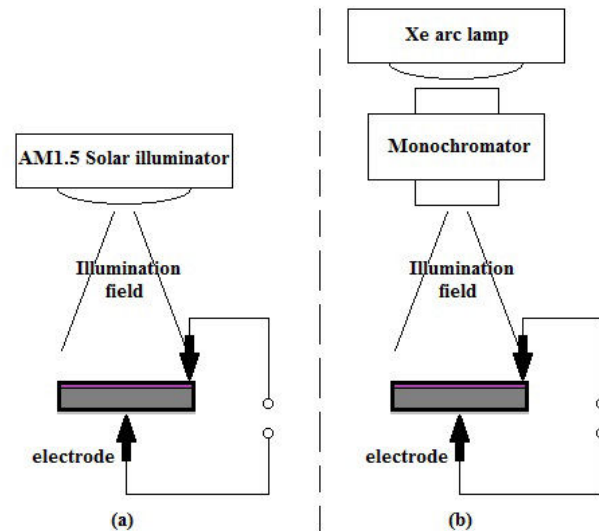


FIGURE 3. Schematic drawing of the measurement system for: (a) AM1.5, and (b) Monochromatic illumination.

through a monochromator. In Figs. 4 and 5, the obtained I-V curves are presented.

As can be seen from Figs. 4 and 5, the samples M1 and M2 have similar response (since are almost twin samples). On the other hand, the sample M3 reaches higher values for the open-circuit voltage and electric power, even when its substrate shows a greater resistivity value (almost 300 fold to the corresponding value to the *p*-type substrates). Possibly, the combination of a thinner buffer layer, and higher values of μ_c and D_c in M3 sample and its substrate, improve the charge transfer in this case.

Table IV summarizes the open-circuit voltages (V_{oc}), the short-circuit currents (I_{sc}), the series resistance (R), the maximum electrical power (W_{max}), and the energy conversion efficiency (η) of the samples, under AM1.5 illumination.

TABLE IV. Results of the Photovoltaic response measurements under homogenous illumination.

	V_{oc}	I_{sc}	R	W_{max}	η
	mV	μA	$\Omega \cdot cm^2$	μW	%
M1	57.8	60.6	230.5	0.9	2.6×10^{-6}
M2	61.2	53.2	290.0	0.8	2.4×10^{-6}
M3	132.9	104.1	287.5	3.6	1.0×10^{-5}

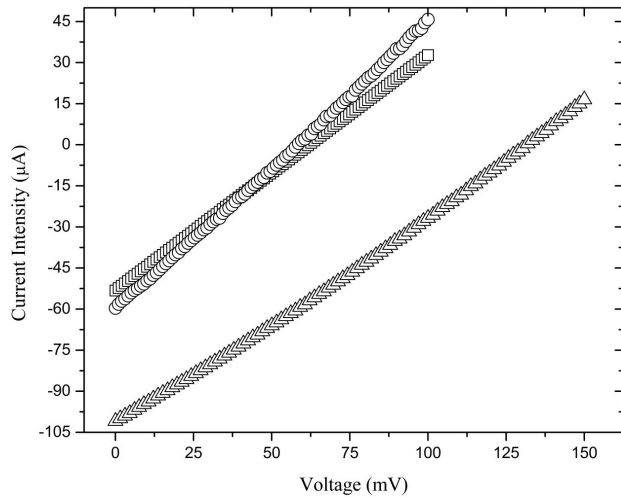


FIGURE 4. I-V curves of samples M1 (empty squares), M2 (empty circles), and M3 (empty triangles).

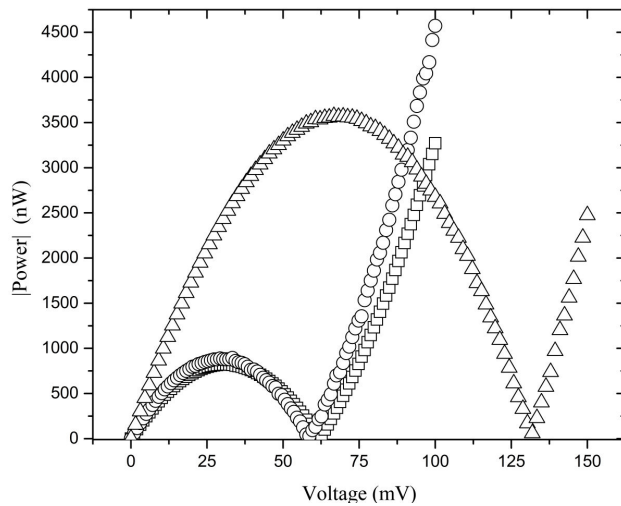


FIGURE 5. Electrical Power of samples M1 (empty squares), M2 (empty circles), and M3 (empty triangles).

The extremely low values of the short-circuit currents and conversion efficiencies can be explained as result of the large values of the thickness of the buffer layer of the samples. Simashevici *et al.* [18] mentioned, in their review work, the great importance of the thickness of the insulator layers to achieving good energy conversion efficiencies in photovoltaic cells. As an example of it, Simashevici *et al.* reports

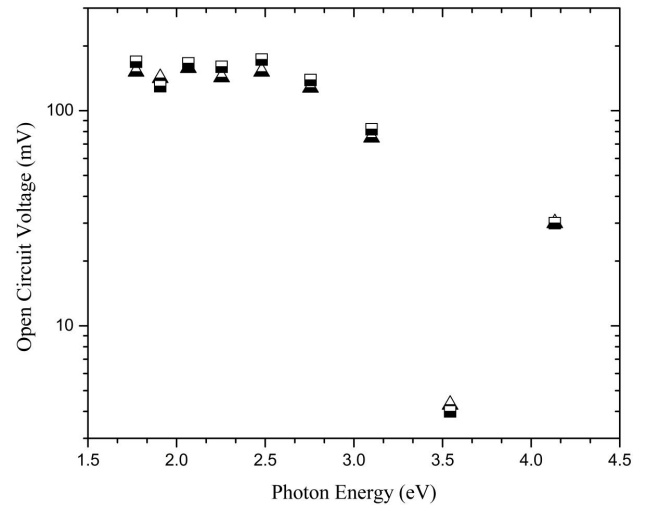


FIGURE 6. Open-circuit voltage, as function of the photon energy: M1 (half-full squares) and M2 (half-full up triangles) samples.

in the aforementioned paper that for $n^+ITO/SiO_2/nSi$ PV cells, the conversion efficiency varies from 1% to 13% for buffer layers with thickness around some tens of Angstroms, being tunneling the principal mechanism for charge transfer. In our case, the thickness of the buffer layers are two orders of magnitude larger, which makes less probably the tunneling of the photogenerated charge carriers.

The results summarized in Table IV supports the idea of a charge transfer mechanism different from tunneling, for the samples under study. It is our impression that the principal charge transfer mechanism is given by the existence of an internal, time-varying displacement electric field, creating a small drift current intensity which reflects in the series resistance values. The origin of such displacement electric field should lie in the diffusion, and in the bulk and surface recombination of the photogenerated charge carriers in GaN and substrate layers. Finally, in Fig. 6, the open-circuit voltage for samples M1 and M2 is shown as function of the photon energy.

As the previous figure indicates, there is a clear dependency of the open-circuit voltage in the photon energy. It can be seen in Fig. 6, that the open-circuit voltage diminishes as the photon energy increases, falling down dramatically for energies close to the GaN band gap energy (3.5 eV), and increasing for higher energies.

For lower energies than 3.1 eV, the typical values for the absorption coefficient of the GaN are in the order of 10^2 cm^{-1} , increasing rapidly (from a minimum value) for photon energy values up to 3.5 eV [19,20]. For the same photon energy range, the substrate increases monotonically their absorption coefficient [21] as the energy increases. Considering the behavior of the absorption coefficients of the GaN and Si layers, for sufficiently small values of the photon energy, the time variations of displacement electric field is due to the recombination of the photogenerated charge carriers in the substrate layer. As the photon energy gets higher, the

open-circuit voltage signal drops because the GaN layer begins to absorb a significant portion of the light, diminishing the light intensity absorbed by the substrate. When the photon energy gets higher values than the GaN band gap energy, more and more photogenerated charge carriers are generated in the GaN layer, and therefore, the open-circuit voltage signal is due to bulk and surface recombination of photogenerated charge carriers in the GaN and Si layers, increasing again the open circuit voltage signal. The spectral response of the open-circuit voltage indicates that these heterostructures could be used as radiation detector.

4. Conclusions

By means of molecular beam epitaxy technique, samples of GaN/AlN/Si were grown under different conditions and substrates. The Hall Effect measurements and I-V curves (in darkness condition) shown that even for unintentional doping of the layers, the charge carrier concentrations reach relatively large values, causing an Ohmic response of the gallium

nitride layer, for the applied current intensity range. Additionally, the I-V curves under AM1.5 illumination shows that the samples form SIS structures with very low energy conversion efficiency, due to the thickness of the buffer layer which does not allow the tunneling of the charge carriers, being probably the presence of a time-varying displacement electric field the most likely charge transport mechanism. It is possible that diminishing the thickness of the buffer layer to some nanometers, the energy conversion efficiency will improve. Further work in this direction is in progress.

Acknowledgments

This work has been supported partially by ICyT-DF (Now SECITI-DF) PICCO10-29 Project, SENER-CONACYT México Project No. 151076, SIP-IPN and COFAA-IPN, México. Finally, the authors thanks the facilities provided by COTEBAL-IPN for the realization of this work. A special acknowledgement is made to M. Ramírez-López, M. Perez-Caro and Y. L. Casallas-Moreno from CINVESTAV-IPN.

-
1. M. Pérez-Caro *et al.*, *Group III-nitrides nanostructures*, In: *Advanced Summer School in Physics 2011* (AIP Conf. Proc. 1420, American Institute of Physics, Melville, New York, 2012) pp 164-168.
 2. Y. Kuwahara, *et al.*, *Appl. Phys. Exp.* **3** (2010) 111001.
 3. Mira Misra, Theodore D. Moustakas, Robert P. Vaudo, Rajminder Singh and Kanai S. Shah, *Photoconducting ultraviolet detectors based on GaN films grown by electron cyclotron resonance molecular beam epitaxy*, In: Richard B. Hoover and Mark B. Williams (eds.) (Proc. SPIE Vol. 2519, *X-Ray and Ultraviolet Sensors and Applications*. San Diego, CA, 1995) pp 78-86.
 4. O. B. Shchekin *et al.*, *Appl. Phys. Lett.* **89** (2006) 071109.
 5. Shuji Nakamura *et al.*, *Jpn. J. Appl. Phys.* **35** (1996) L74.
 6. R. Graupner, QiYe, T. Warwick, and E. Bournet-Courchesne, *J. Cryst. Growth* **217** (2000) 55.
 7. M. Tamura and M. López-López, *Superficies y Vacío* **13** (2001) 80.
 8. Nikishin *et al.*, *MRS Internet J. Nitride Semicond. Res.* **5S1** (2000) W8.3.
 9. M.S.N.M. Brandt, N.M. Johnsonn, R.J. Molnar, R. Singh, and T.D. Moustakas, *Appl. Phys. Lett.* **64** (1994) 2264.
 10. C.W. Chin, F.K. Yam, K.P. Beh, Z. Hassan, M.A. Ahmad, Y. Yusof, S.K. Mohd Bakhori, *Thin Solid Films* **520** (2011) 756.
 11. Junqiao Wu, *J. Appl. Phys.* **106** (2009) 011101.
 12. S.J. Pearton *et al.*, *J. Appl. Phys.* **93** (2003) 1.
 13. S. Pezzagna, J. Brault, M. Leroux, J. Massies and M. de Micheli, *J. Appl. Phys.* **103** (2008) 123112.
 14. Naser M. Ahmed, Zaliman Sauli, Uda Hashim and Yarub Al-Douri, *Int. J. Nanoelectronics and Materials* **2** (2009) 189.
 15. L.J. van der Pauw, *Phillips Res. Repts.* **13** (1958) 1.
 16. D.L. Rode and D K Gaskill, *Appl. Phys. Lett.* **6** (1995) 1972.
 17. M. Asif Khan, M.S. Shur and Q. Chen, *Appl. Phys. Lett.* **68** (1996) 3022.
 18. Alexei Simashevici, Dormidont Serban and Leonid Bruc, *Solar Cells on the Base of Semiconductor-Insulator-Semiconductor Structures*, In: *Solar Cells-Silicon Wafer-Based Technologies* (ed.) Prof. Leonid A. Kosyachenko (JanezaTrdine 9, 51000, Rijeka, Croatia: InTech, 2011) pp. 299-332.
 19. J. F. Muth *et al.*, *Appl. Phys. Lett.* **71** (1997) 2572.
 20. O. Ambacher, W. Rieger, P. Ansmann, H. Angerer, T. D. Moustakas, M. Stutzman, *Sol. State Commun.* **97** (1996) 365.
 21. S.M. Sze, *Physics of Semiconductor Devices* (John Wiley and Sons, N.Y, 1981).